Commun. Comput. Chem.
doi: 10.4208/cicc.2016.v4.n1.3

Vol.4, No.1, pp.24-35
June 2016

REGULAR ARTICLE

Theoretical study of the reactivity between RuIV(O) complexes and their inverted-isomers

Peng Zhang[1], Zhe Tang[2], Yi Wang [2*]

[1]*School of Mechanical Engineering and Automation, Dalian Polytechnic University, Dalian 116034, P. R.China;*

[2]*School of Biological Engineering, Dalian Polytechnic University, Dalian 116034, P. R.China*

Received 13 May 2016; Accepted (in revised version) 23 June 2016

Abstract: Density functional theory calculations were carried out to investigate geometric and electronic structures and mechanisms for hydrogen abstraction from cyclohexane for six non-heme ruthenium-oxo complexes [RuIV(O)(TMC)(X)]+ (1-Ru-X) and their inverted isomers [RuIV(X)(TMC)(O)]+ (2-Ru-X; Scheme 1; where TMC is 1,4,8,11-tetramethyl-1,4,8,11-tetraazacyclotetradecane; X = TF-, N3- and SR-). The calculations offer a mechanistic view and reveal the following features: (a) all six ruthenium (IV)-oxo complexes possess a triplet ground spin state, and the quintet spin state is too high to participate in the reaction. (b) The six complexes react with cyclohexane via a single-state reactivity pattern only on the triplet spin surface. (c) A more negative ΔqCT results in a greater tunneling contribution effect. (d) At the B2//B1+ZPE level, the relative reactivity of the hydrogen abstraction follows the trend: 1-Ru-SR > 1-Ru-N3 > 1-Ru-TF and 2-Ru-SR > 2-Ru-N3 > 2-Ru-TF. The relative reactivity of 2-Ru-X is greater than that of 1-Ru-X. (e) The effect of the tunneling contribution is higher for 1-Ru-X than for 2-Ru-X; with the tunneling correction, the relative reactivities between 1-Ru-X and 2-Ru-X change and the trend becomes: 2-Ru-TF > 1-Ru-TF, 2-Ru-N3 > 1-Ru-N3 and 2-Ru-SR < 1-Ru-SR.

AMS subject classifications: 74E40, 74F45

Key Words: Non-heme; Ruthenium-oxo; Steric Hindrance; H-abstraction; Density functional theory

Introduction

* Corresponding author. *Email address:* wangyi@dlpu.edu.cn, Fax: +86 0411-86323646

Oxygen-activating enzymes with mononuclear non-heme iron active sites participate in many metabolically important reactions that have environmental, pharmaceutical, and medical significance [1]. These enzymes activate dioxygen, with the aid of a two-electron sacrificial reductant, to generate a highly reactive oxoiron (IV) species, which is proposed to be the active intermediate in the oxidation of a number of important biomolecules [2]. To data, many mononuclear non-heme iron complexes have been synthesized as chemical models of the non-heme iron enzymes [3]. In the non-heme systems, the axial and equatorial ligands to the metal-oxo moiety on the reactivities of the non-heme iron(IV)-oxo complexes have attracted much attention in the electron-transfer and oxidation reactions[4-6].

In 2003, the first structurally characterized synthetic oxoiron (IV) complex, [FeIV(O)(TMC)(NCMe)]2+ has been reported (where TMC is 1,4,8,11-tetramethyl-1,4,8,11-tetraazacyclotetradecane) [7]. In 2005, the effect of a thiolate ligand on the catalytic properties of non-heme oxoiron complexes was studied [8, 9]. Since then, many studies of the analogous complexes have been carried out [4,10-12]. An inverted-isomers, [FeIV(NCMe)(TMC)(O)]2+, of [FeIV(O)(TMC)(NCMe)]2+ , in which the oxo group binds to the site syn to the four N-methyl groups, was synthesized by Ray et al [13]. The different reactivities between the [FeIV(O)(TMC)(X)]n+ and their inverted-isomers, and the factors, which can influence the reactivity of C-H hydroxylation and C=C epoxidation by [FeIV(X)(TMC)(O)]n+ have been calculated [14].

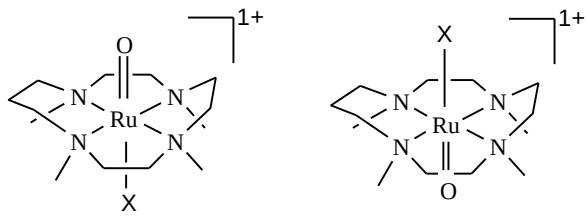

1-Ru-X 2-Ru-X

X=TF, N3

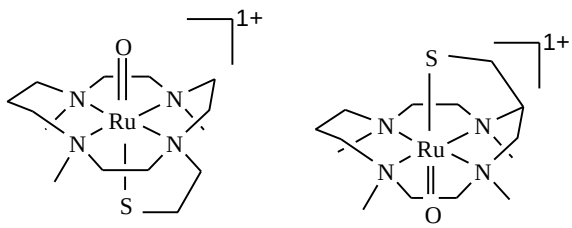

1-Ru-SR 2-Ru-SR

1-Ru-SR: SR is appended to an N-atom through an ethyl linker
2-Ru-SR: SR is attached to a methylene linker in the TMC backbone

Scheme 1 Structures of 1-Ru-X and 2-Ru-X.

High-valent ruthenium-oxo complexes of non-heme ligands have also been invoked as active oxidants in catalytic oxidation [15-18]. The ruthenium analogue of [FeIV(O)(TMC)(NCMe)]2+, [RuIV(O)(TMC)(NCMe)]2+ was first reported in 1985 [19]. The reactivity of [FeIV(O)(TMC)(NCMe)]2+ and [RuIV(O)(TMC)(NCMe)]2+ in the hydrogen-abstraction reactions was investigated by Dhuri et al [20], while the reactivity of its inverted-isomers, [FeIV(NCMe)(TMC)(O)]2+ and [RuIV(NCMe)(TMC)(O)]2+ had been studied by Wang et al [21]. As shown in the earlier work [20,21], in the C-H bond activation reactions, the RuIV-oxo complex prefers the single-state reactivity pattern.

A study of FeIV(O) and its inverted-isomers revealed that the reactivity is affected significantly by axial ligands and the steric hindrance of the equatorial ligand [14]. To determine whether the same effect can influence the electronic properties and reactivity patterns of the ruthenium (Ru) (IV)-oxo complexes, we have studied the Ru(IV)-oxo species, which have the same equatorial ligand and different anion axial ligand ([RuIV(O)(TMC)(TF)]+, [RuIV(O)(TMC)(N3)]+ and [RuIV(O)(TMC)(SR)]+), and their inverted isomers species ([RuIV(TF)(TMC)(O)]+, [RuIV(N3)(TMC)(O)]+ and [RuIV(SR)(TMC)(O)]+).

Computational methods

Standard methods

We considered the triplet and quintet spin states for Ru(IV)-oxo species ([RuIV(O)(TMC)(TF)]+, [RuIV(O)(TMC)(N3)]+ and [RuIV(O)(TMC)(SR)]+) and their inverted isomers ([RuIV(TF)(TMC)(O)]+, [RuIV(N3)(TMC)(O)]+ and [RuIV(SR)(TMC)(O)]+). DFT calculations were performed with the Gaussian 09 suite of a quantum chemical package [22], and the spin-unrestricted Becke, three-parameter, Lee-Yang-Parr (B3LYP) functional [23] as the method of choice. The geometries for the six non-heme ruthenium-oxo complexes were fully optimized without symmetry constraints. The Lanl2DZ basis set [24] was used for ruthenium, moreover 6-31G**[24c, 25] for the other atoms (B1 in brief). Single-point calculations on the Lanl2DZ-optimized geometry were performed with a higher basis set def2TZVP [26], B2 in brief. All optimizations and single-point calculations were performed with solvation included using the self-consistent reaction field (SCRF) calculations, within the polarizable continuum model (PCM) [27]. All local minima only have real frequencies, whereas the transition states have one imaginary frequency for the correct mode.

Tunneling Corrections

Eckart tunneling calculations were performed using TheRate Program [28]. Due to the tunneling, the transmission coefficient κ, is calculated by integrating of the barrier "penetration" probability as a Boltzmann-averaged function of the energy [29]. The effect of the transmission coefficient on the barrier is calculated by the equation [12]:

$$\Delta\Delta E^{\#}_{tun} = -RT\ln\kappa(T) \qquad \text{eq (1)}$$

where R denotes the universal gas constant and T is the absolute temperature. Generally, the experimental rate data were collected at 273K.

Results and Discussion

Properties of the six RuIV(O) complexes

Figure 1 shows the optimized structures of $[Ru^{IV}(O)(TMC)(X)]^{+}$ with X = TF^{-}, $N3^{-}$ and SR^{-} and their inverted isomers $[Ru^{IV}(X)(TMC)(O)]^{+}$, and the corresponding energies relative to the triplet spin state at the B2//B1(B2//B1+ZPE) level. At the B2//B1+ZPE level, the triplet spin state is energetically favored by 42.6, 41.6, 39.8, 45.3, 43.5 and 42.8 kcal/mol below the quintet spin state for 1-Ru-TF, 1-Ru-N3, 1-Ru-SR, 2-Ru-TF, 2-Ru-N3 and 2-Ru-SR, respectively. The energy gap between the triplet and quintet spin states for the 1-Ru-X complex is lower than the corresponding inverted-isomer (2-Ru-X). Regardless of whether 1-Ru-X or 2-Ru-X is present, the greater electron-releasing ligand exhibits a lower triplet-quintet energy gap. For the Ru(IV)-oxo complexes of non-heme ligands, the quintet spin state is too high to enable participation in the reaction; hence the reactions are single-state and only involve the triplet spin state.

Figure 1: The optimized structures and the van der Waals radii space-filling models derived from geometry-optimized structures. The relative energies (kcal/mol) for the quintet spin state are relative to the triplet spin state at the B2//B1 (B2//B1+ZPE) level.

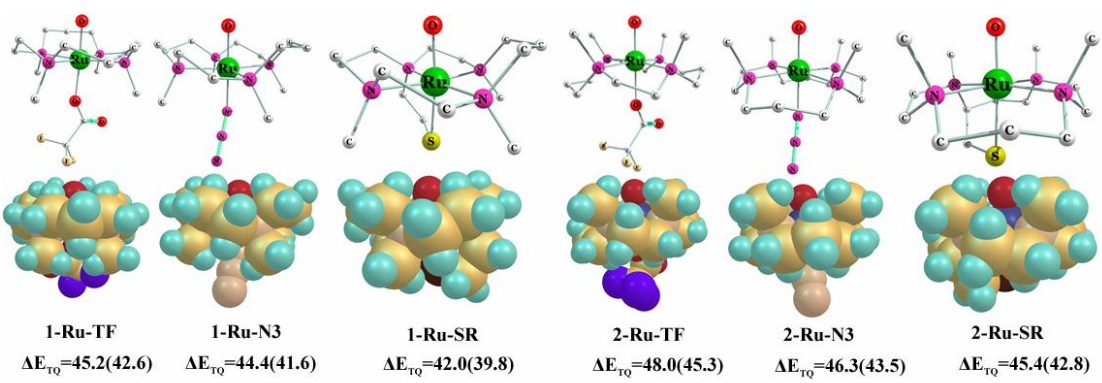

The geometric and electronic details are listed in **Table 1**. For 1-Ru-X, the Ru-O distances are 1.777–1.811Å, whereas the Ru-X distances are 2.133–2.488 Å. In contrast with the 1-Ru-X complexes, because of the oxo location *syn* to the four *N*-methyl groups, 2-Ru-X has shorter Ru-O distances and longer Ru-X bond lengths. Δq_{CT} indicates the electron-donating ability of the different axial ligands. As reported previously [12], when more charge is transferred from the axial ligand to the metal center, the axial ligand is more electron-donating. Thus, the Δq_{CT} value (**Table 1**) shows that TF is the least electron-releasing ligand, whereas SR is the most electron-donating axial ligand. In the triplet spin state, for 1-Ru-X, the Ru-O distance is longest in 1-Ru-SR, and shortest in 1-Ru-TF, whereas the corresponding distances have the same trend for 2-Ru-X. The Wiberg bond order of RuO-X is strongest in 1-Ru-SR among the three 1-Ru-X complexes, and for 2-Ru-X, the Wiberg bond order between the RuO fragment and the axial ligand is strongest in 2-Ru-SR. Because of the greater steric hindrance between the equatorial and axial ligands of 2-Ru-X, the bond order between the RuO fragment and the axial ligand in 1-Ru-X is stronger than that of the corresponding bond order in 2-Ru-X.

Table 1 Key geometric features (lengths in Å, angles in °), parameters of the electronic structures, the transmission coefficients for H-tunneling at the 273 K and the barrier lowering quantities of UB3LYP/B1-optimized structures for the triplet spin state.

	Bond Length		Angle	Bond Order[a,b]		Charges[a,c]	Δq_{CT}	$\kappa(T)$	$\Delta\Delta E^{\neq}_{tun}$
	Ru=O	Ru-X	Ru-O-H	Ru=O	RuO-X	O			
1-Ru-TF	1.777	2.152	95.58	1.529	0.535	-0.279	-0.41	8.843×10	-2.4
1-Ru-N3	1.793	2.133	95.61	1.460	0.649	-0.301	-0.44	1.354×10^2	-2.7
1-Ru-SR	1.811	2.488	95.36	1.393	1.033	-0.310	-0.76	2.966×10^2	-3.1
2-Ru-TF	1.767	2.221	92.05	1.584	0.490	-0.288	-0.43	3.813×10	-2.0
2-Ru-N3	1.780	2.190	92.25	1.528	0.624	-0.309	-0.44	5.636×10	-2.2
2-Ru-SR	1.798	2.543	91.73	1.468	0.948	-0.324	-0.73	9.274×10	-2.5

a The bond order analysis and the charges are calculated by the Multiwfn software [33,34]

b The bond order is the Wiberg bond order in Löwdin orthogonalized basis

c The charges is the Hirshfeld charges

Hydrogen-abstraction mechanism

For the hydrogen abstraction reaction, in all mechanisms, the reactants form a reactant cluster, followed by a transition state that leads to an intermediate [30]. **Figure 2** shows energy profiles for the hydrogen abstraction from cyclohexane by the six Ru^{IV}-oxo complexes. **Figure 3** shows geometric details of the transition states for the triplet spin states.

Hydrogen abstraction by 1-Ru-X

Figure 2 shows that hydrogen abstraction is exothermic, exhibits single-state-reaction and only passes via the triplet spin surface. As shown in **Figure 2**, for the 1-Ru-X complexes, the activation energies at the UB3LYP/B2+ZPE level are 34.4, 32.7 and 29.0 kcal/mol for 1-Ru-TF, 1-Ru-N3 and 1-Ru-SR, respectively. The tunneling effect correction leads to a decrease in the effective barriers, which become 32.0, 30.0 and 25.9 kcal/mol, respectively.

The structures of the ^3TS_H in **Figure 3** show that CH attacks the oxo group from the side; hence the Fe-O-H angles are ~130°. The C-H distances for the three 1-Ru-X complexes are 1.429, 1.411 and 1.383 Å, respectively, whereas the O-H distances of ^3TS_H are 1.162, 1.169 and 1.185 Å, respectively. Thus, for 1-Ru-X with the same equatorial ligand, a greater electron-releasing axial ligand yields a longer O-H and shorter C-H distance, which means that ^3TS_H will form earliest for 1-Ru-SR.

Hydrogen abstraction by 2-Ru-X

The calculated reaction energies between the 2-Ru-X and CH are shown in **Figure 2**. Similar to the reactivities for 1-Ru-X, for the hydrogen abstraction, in the triplet spin state, at the UB3LYP/B2+ZPE level, the reaction barriers are 32.6, 31.6 and 28.9 kcal/mol, for 2-Ru-TF, 2-Ru-N3 and 2-Ru-SR, respectively. The barriers decrease with tunneling and become 30.6, 29.4 and 26.4 kcal/mol, respectively. **Figure 3** presents geometric parameters of the transition state for ^3TS_H along the reaction pathways. The O-H lengths are 1.152, 1.155 and 1.162 Å and the C-H lengths are 1.428, 1.420 and 1.404 Å, respectively. 2-Ru-SR is the most reactive of the three complexes with the longest O-H and shortest C-H distance.

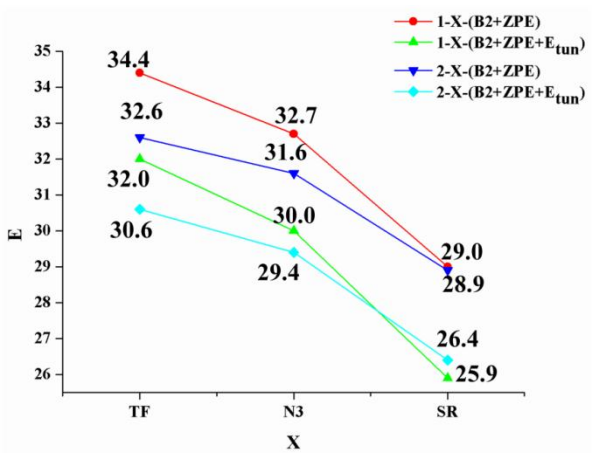

Figure 2: The relative energy barriers of the hydrogen-abstraction for the ruthenium-oxo complexes and their inverted-isomers.

Electron donation of axial ligands

Δq_{CT} is defined as the electron ability of the different axial ligands. A larger number of charges transferred from the axial ligand to the iron center results in a larger $|\Delta q_{CT}|$. Thus, TF is the least electron-releasing ligand, whereas SR is the most electron-donating axial ligand. As shown in **Table 2** and **Figure 2**, when Δq_{CT} is more negative, the difference in reaction barriers between 1-Ru-X and 2-Ru-X decreases.

Steric hindrance of equatorial ligand

Table 1 lists the Wiberg bond order between the FeO and axial ligand fragments, and also between the Fe and O units. Because of the significant steric hindrance of the TMC ligand with the axial ligand, the bond strengths between the two fragments are weaker for the 2-Ru-X than for the corresponding 1-Ru-X; whereas the lower steric hindrance of the TMC ligand with the RuO unit results in a stronger bond strength between the two fragments for the 2-Ru-X than that of 1-Ru-X for the same axial ligand. Because the anion axial ligand is close to the RuO unit, the steric hindrance of the TMC ligand with the axial ligand has little effect on the relative reactivity of 1-Ru-X and 2-Ru-X. As shown in **Figure 3**, for the six non-heme ruthenium complexes, the Ru-O-H angles are ~130°, ^3TS_H follows the π^* trajectory and CH will attack the oxo group from the side, which is dominated by the overlap of π^*_{xz} and σ_{CH} orbitals. Thus, the steric hindrance between the TMC ligand and the RuO unit are very important. To understand the steric hindrance effect on the relative reactivities between 1-Ru-X and 2-Ru-X, we have tested the most important key structural parameter (**Table 1**, ∠Ru-O-H). The obtuse ∠H-O-Ru angles place the oxo group of the six $Ru^{IV}O$ complexes in the cavity because of the increased steric hindrance between the equatorial ligand and the RuO unit. **Figure 2** shows that at the B2//B1+ZPE level, the relative reactivity follows the order: 2-TF-Ru > 1-TF-Ru, 2-N3-Ru > 1-N3-Ru and 2-SR-Ru > 1-SR-Ru.

Tunneling effect on hydrogen abstraction reaction

It is important to consider the effect of tunneling on the effective reaction barrier. Depending on the transmission coefficient as specified in Eq. 1, tunneling "through" the barrier reduces the coefficient by $\Delta\Delta E^{\#}_{tun}$ [12, 31, 32]. As listed in Table 1, after adding a tunneling correction, the reaction barrier should be reduced. For the 1-Ru-X system, $|\Delta\Delta E^{\#}_{tun}|$ is larger than the corresponding correction energy in the 2-Ru-X system. Moreover, the tunneling effect depends on the electron-donating axial ligand; a more negative Δq_{CT} results in a larger $|\Delta\Delta E^{\#}_{tun}|$. At the B2//B1+ZPE+$\Delta\Delta E^{\#}_{tun}$ level, the reaction barrier is 32.0, 30.0, 25.9, 30.6, 29.4

and 26.4 kcal/mol for 1-Ru-TF, 1-Ru-N3, 1-Ru-SR, 2-Ru-TF, 2-Ru-N3 and 2-Ru-SR, respectively. The relative reactivity of 1-Ru-X follows the order: 1-Ru-SR > 1-Ru-N3 > 1-Ru-TF. For 2-Ru-X, the relative reactivity follows the order: 2-Ru-SR > 2-Ru-N3 > 2-Ru-TF, which have the same trend as the $[Fe^{IV}(O)(TMC)(X)]^+$ (X=TF^-, $N3^-$ and SR^-) complexes and their inverted isomers. Thus, except for 2-Ru-SR, the relative reactivity of 2-Ru-X is greater than the corresponding 1-Ru-X, which follows the trend: 2-TF-Ru > 1-TF-Ru, 2-N3-Ru > 1-N3-Ru and 2-SR-Ru < 1-SR-Ru.

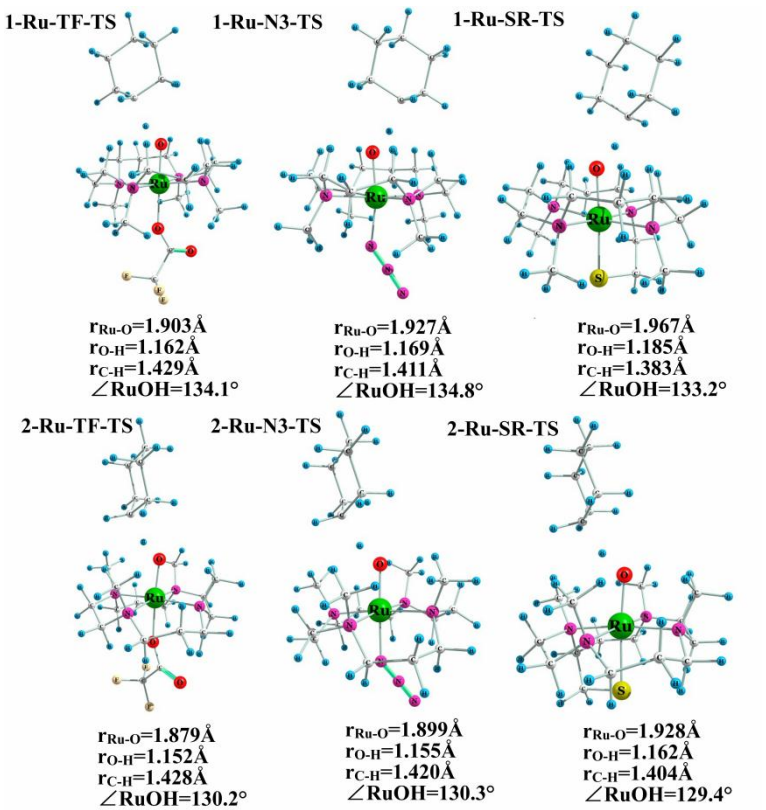

Figure 3: Geometric details of the hydrogen-abstraction transition states at B1 level in the triplet spin state.

Conclusion

The UB3LYP calculations show that the non-heme ruthenium-oxo complexes addressed in this study possess triplet ground states and the mechanism of hydrogen abstraction is a single-state reaction. A comparison of the 1-Ru-X and 2-Ru-X structures shows that 2-Ru-X has a shorter Ru-O distance and longer Ru-X bond length because of the oxo location *syn* to the four *N*-methyl groups. The reactivity shows some dependence on steric hindrance of the equatorial ligand with the RuO unit. Our results also show that a better axial ligand electron

donor yields a greater tunneling reaction barrier correction. $|\Delta\Delta E^{\#}_{tun}|$ of the 1-Ru-X system is larger than the corresponding correction energy in the 2-Ru-X system. Thus, for the hydrogen abstraction reaction, the relative reactivity of 1-Ru-X follows the trend: 1-Ru-SR > 1-Ru-N3 > 1-Ru-TF, whereas for 2-Ru-X, the trend is: 2-Ru-SR > 2-Ru-N3 > 2-Ru-TF. At the B2//B1+ZPE+$\Delta\Delta E^{\#}_{tun}$ level, in addition to 2-Ru-SR, the relative reactivity of 2-Ru-X is greater than the corresponding 1-Ru-X.

Acknowledgements

This work was supported by the Public science and technology research funds projects of ocean (201505029), Funded by National Engineering Research Center of Seafood (2012FU125X03), Funded by Key University Science and Technology Platform of Liaoning Province (No. 2011-191). The results of quantum chemical calculations described in this paper were obtained on the homemade Linux cluster of group 1101, Dalian Institute of Chemical Physics.

Reference:

[1] L. Que Jr, R. Y. N. Ho, Dioxygen activation by enzymes with mononuclear non-heme iron active sites. Chem. Rev, 96 (1996), 2607-2624.

[2] M. Puri, L. Que Jr, Toward the synthesis of more reactive S=2 non-heme oxoiron(IV) complexes. Acc. Chem. Res, 48 (2015), 2443-2452.

[3] Y. Suh, M. S. Seo, K. M. Kim, Y. S. Kim, H. G. Jang, T. Tosha, T. Kitagawa, J. Kim, W. Nam, Nonheme iron(II) complexes of macrocyclic ligands in the generation of oxoiron(IV) complexes and the catalytic epoxidation of olefins. J. Inorg. BioChem, 100 (2006), 627-633.

[4] C. V. Sastri, J. Lee, K. Oh, Y. J. Lee, J. Lee, T. A. Jackson, K. Ray, H. Hirao, W. Shin, J.A. Halfen, J. Kim, L. Que Jr, S. Shaik, W. Nam, Axial ligand tuning of a nonheme iron(IV)-oxo unit for hydrogen atom abstraction. Proc. Natl. Acad. Sci, 104 (2007), 19181-19186.

[5] Y. M. Zhou, X. P. Shan, R. Mas-Balleste, M. R. Bukowski, A. Stubna, M. Chakrabarti, L. Slominski, J. A. Halfen, E. Munck, L. Que Jr, Contrasting cis and trans effects on the reactivity of nonheme oxoiron(IV) complexes. Angew. Chem. Int. Ed, 47 (2008), 1896-1899.

[6] W. Nam, Y. M. Lee, S. Fukuzumi, Tuning reactivity and mechanism in oxidation reactions by mononuclear nonheme iron(IV)-oxo complexes. Acc. Chem. Res, 47 (2014), 1146-1154.

[7] J. U. Rohde, J. H. In, M. H. Lim, W. W. Brennessel, M. R. Bukowski, A. Stubna, E. Munck, W. Nam, L. Que Jr, Crystallographic and spectroscopic characterization of a nonheme Fe(IV)=O Complex. Science, 299 (2003), 1037-1039.

[8] M. R. Bukowski, K. D. Koehntop, A. Stubna, E. L. Bominaar, J. A. Halfen, E. Munck, W. Nam, L. Que Jr, A thiolate-ligated nonheme oxoiron(IV) complex relevant to cytochrome P450. Science, 310 (2005), 1000-1002.

[9] S. P. de Visser, What factors influence the ratio of C-H hydroxylation versus C=C epoxidation by a nonheme cytochrome P450 biomimetic? J. Am. Chem. Soc, 128 (2006), 15809-15818.

[10] H. Hirao, L. Que Jr, W. Nam, S. Shaik, A two-state reactivity rationale for counterintuitive axial ligand effects on the C-H activation reactivity of nonheme Fe-IV = O oxidants Chem. Eur. J, 14 (2008), 1740-1756.

[11] T. A. Jackson, J. U. Rohde, M. S. Seo, C. V. Sastri, R. DeHont, A. Stubna, T. Ohta, T. Kitagawa, E. Munck, W. Nam, L. Que Jr, Axial ligand effects on the geometric and electronic structures of nonheme oxoiron(IV) complexes. J. Am. Chem. Soc, 130 (2008), 12394-12407.

[12] D. Mandal, R. Ramanan, D. Usharani, D. Janardanan, B. J. Wang, S. Shaik, How does tunneling contribute to counterintuitive H-abstraction reactivity of nonheme Fe(IV)O oxidants with alkanes? J. Am. Chem. Soc, 137 (2015), 722-733.

[13] K. Ray, J. England, A. T. Fiedler, M. Martinho, E. Munck, L. Que Jr, An inverted and more oxidizing isomer of [Fe(IV)(O)(tmc)(NCCH(3))](2+). Angew. Chem. Int. Ed, 47 (2008), 8068-8071.

[14] Y. Wang, Y. Liu, K. Yang, Z. W. He, J. Tian, X. Fei, H. Guo, Y. Wang, What factors influence the reactivity of C-H hydroxylation and C=C epoxidation by [Fe-IV(L-ax)(1,4,8,11-tetramethyl-1,4,8,11-tetraazacyclotetradecane)(O)](n+). J. Biol. Inorg. Chem, 20 (2015), 1123-1134.

[15] M. Pagliaro, S. Campestrini, R. Ciriminna, Ru-based oxidation catalysis. Chem. Soc. Rev, 34 (2005), 837-845.

[16] S. L. F. Chan, Y. H. Kan, K. L. Yip, J. S. Huang, C. M. Che, Ruthenium complexes of 1,4,7-trimethyl-1,4,7-triazacyclononane for atom and group transfer reactions. Coord. Chem. Rev, 255 (2011), 899-919.

[17] T. Ishizuka, S. Ohzu, T. Kojima, Oxidation of organic substrates with Ru-IV=O complexes formed by proton-coupled electron transfer. Synlett, 25 (2014), 1667-1679.

[18] S. N. Dhui, K. B. Cho, Y. M. Lee, S. Y. Shin, J. H. Kim, D. Mandal, S. Shaik, W. Nam, Interplay of experiment and theory in elucidating mechanisms of oxidation reactions by a nonheme (RuO)-O-IV complex. J. Am. Chem. Soc, 137 (2015), 8623-8632.

[19] C. M. Che, K. Y. Wong, T. C. W. Mak, Characterization of a high-valent ruthenyl (RuIV=O) cation stabilized by the macrocyclic 1,4,8,11-tetramethyl-1,4,8,11-tetra-azacyclotetradecane (TMC) ligand - crystal and molecular-structure of trans-[RuIV(TMC)O(MeCN)][PF6]2. J. Chem. Soc. Chem. Commun, (1985), 546-548.

[20] S. N. Dhuri, M. S. Seo, Y. M. Lee, H. Hirao, Y. Wang, W. Nam, S. Shaik, Experiment and theory reveal the fundamental difference between two-state and single-state reactivity patterns in nonheme Fe-IV=O versus Ru-IV=O oxidants. Angew. Chem. Int. Ed, 47 (2008), 3356-3359.

[21] Y. Wang, K. L. Han, Steric hindrance effect of the equatorial ligand on Fe(IV)O and Ru(IV)O complexes: a density functional study. J. Biol. Inorg. Chem, 15 (2010), 351-359.

[22] M.J. Frisch, G.W. Trucks, H.B. Schlegel, G.E. Scuseria, M.A. Robb, J.R. Cheeseman, G. Scalmani, V. Barone, B. Mennucci, G.A. Petersson, H. Nakatsuji, M .Caricato, X. Li, H.P. Hratchian, A.F. Izmaylov, J.

Bloino, G. Zheng, J.L. Sonnenberg, M. Hada, M. Ehara, K. Toyota, R. Fukuda, J. Hasegawa, M. Ishida, T. Nakajima, Y. Honda, O. Kitao, H. Nakai, T. Vreven, J.A. Montgomery, J.E. Peralta, F. Ogliaro, M. Bearpark, J.J. Heyd, J. E. Brothers, K.N. Kudin, V.N. Staroverov, R. Kobayashi, J. Normand, K. Raghavachari, A. Rendell, J.C. Burant, S.S. Iyengar, J. Tomasi, M. Cossi, N. Rega, J.M. Millam, M. Klene, J.E. Knox, J.B. Cross,V. Bakken, C. Adamo, J. Jaramillo, R. Gomperts, R.E. Stratmann, O. Yazyev, A.J. Austin, R. Cammi, C. Pomelli, J.W. Ochterski, R.L. Martin, K. Morokuma, V.G. Zakrzewski, G.A. Voth, P. Salvador, J.J. Dannenberg, S. Dapprich, A.D. Daniels, O. Farkas, J.B. Foresman, J.V. Ortiz, J. Cioslowski, D.J. Fox, Gaussian 09, revision D.01; Gaussian, Inc.: Wallingford, CT, 2009.

[23] (a) A. D. Becke, Density‐functional thermochemistry. I. The effect of the exchange‐only gradient correction. J. Chem. Phys, 96 (1992), 2155-2160. (b) A. D. Becke, Density-functional thermochemistry.2. the effect of the perdew-wang generalized-gradient correlation correction. J. Chem. Phys, 97 (1992), 9173-9177. (c) A. D. Becke, Density-functional thermochemistry .3. the role of exact exchange. J. Chem. Phys, 98 (1993), 5648-5652. (d) C. Lee, W. Yang, R.G. Parr, Development of the colle-salvetti correlation-energy formula into a functional of the electron-density. Phys. Rev. B, 37(1988), 785-789.

[24] (a) T. H. Dunning Jr, P. J. Hay, HF III. Eds. Schaefer, Modern Theoretical Chemistry, Plenum, New York, 1976, 1. (b) P. J. Hay, W. R. Wadt, Abinitio effective core potentials for molecular calculations - potentials for the transition-metal atoms Sc to Hg. J. Chem. Phys, 82 (1985), 270-283. (c) J. P. Hay, W. R. Wadt, Abinitio effective core potentials for molecular calculations - potentials for K to Au including the outermost core orbitals. J. Chem. Phys, 82 (1985), 299-310.

[25] R. A. Friesner, R. B. Murphy, M. D. Beachy, M. N. Ringnalda, W. T. Pollard, B. D. Dunietz, Y. X. Cao, Correlated ab initio electronic structure calculations for large molecules. J. Chem. Phys. A,103 (1999), 1913-1928.

[26] (a) A. Schafer, H. Horn, R. Ahlrichs, Fully optimized contracted gaussian-basis sets for atoms Li to Kr. J. Chem. Phys, 97 (1992), 2571-2577. (b) A. Schafer, C. Huber, R. Ahlrichs, Fully optimized contracted gaussian-basis sets of triple zeta valence quality for atoms Li to Kr. J. Chem. Phys,100 (1994), 5829-5835.

[27] J. Tomasi, B. Mennucci, R. Cammi, Quantum mechanical continuum solvation models. Chem. Rev, 105 (2005), 2999-3094.

[28] (a) W. T. Duncan, R. L. Bell, T. N. Truong, TheRate: Program for ab initio direct dynamics calculations of thermal and vibrational-state-selected rate constants. J. Comput. Chem, 19 (1998), 1039-1052. (b) S. W. Zhang, T. N. Truong, VKLab version 1.0. University of Utah, Salt Lake City.

[29] C. Eckart, The penetration of a potential barrier by electrons. Phys. Rev, 35 (1930), 1303-1309.

[30] H. Hirao, D. Kumar, L. Que Jr, Two-state reactivity in alkane hydroxylation by non-heme iron-oxo complexes. J. Am. Chem. Soc, 128 (2006), 8590-8606.

[31] D. Ley, D. Gerbig, P. R. Schreiner, Tunnelling control of chemical reactions - the organic chemist's perspective. Org. Biomol. Chem, 10 (2012), 3781-3790.

[32] P. R. Schreiner, H. P. Reisenauer, D. Ley, D. Gerbig, C. H. Wu, W. D. Allen, Methylhydroxycarbene: Tunneling Control of a Chemical Reaction. Science, 322 (2011), 1300-1303.

[32] T. Lu, F. W. Chen, Multiwfn: A multifunctional wavefunction analyzer. J. Comp. Chem, 33 (2012), 580-592.

[33] T. Lu, F. W. Chen, Calculation of Molecular Orbital Composition. Acta. Chim. Sinica, 69 (2011), 2393-2406.